Effect of hybrid nano particle reinforcements on fractographic, mechanical and wear behavior of Al6061 alloy composites manufactured by ultrasonic assisted stir casting technique

Annapoorna Krishnappa
Dept. of Mechanical Eng., RNS Institute of Technology, Visvesvaraya Technological University, India
annapoorna.apk@gmail.com, http://orcid.org/0000-0003-2543-4801

Shobha Ramesh
Dept. of Industrial Eng. and Management, Ramaiah Institute of Technology, Bengaluru, Karnataka, India
shobhamtech@gmail.com, http://orcid.org/0000-0003-0210-3540

Bharath Vedashantha Murthy
Dept. of Mechanical Eng., RNS Institute of Technology, Visvesvaraya Technological University, India,
bharathv88@gmail.com, http://orcid.org/0000-0001-6765-4728

Rajanna Siddagangappa
Dept. of Mechanical Eng., Government Engineering College, Mosale Hosahalli, Karnataka, India
rajanna.cit@gmail.com, http://orcid.org/0000-0001-9209-5104

Srimadhu Ashokkumar
Trelleborg Sealing Solutions, Bengaluru, Karnataka, India
srimadhua@gmail.com, http://orcid.org/0009-0002-7671-2381

Madeva Nagaral
Aircraft Research and Design Centre, Hindustan Aeronautics Limited, Bangalore 560037, Karnataka, India
madev.nagaral@gmail.com, http://orcid.org/0000-0002-8248-7603

Virupaxi Auradi
Department of Mechanical Engineering, Siddaganga Institute of Technology, Tumakuru-572103, Karnataka, India
vsauradi@gmail.com, http://orcid.org/0000-0001-6549-6340

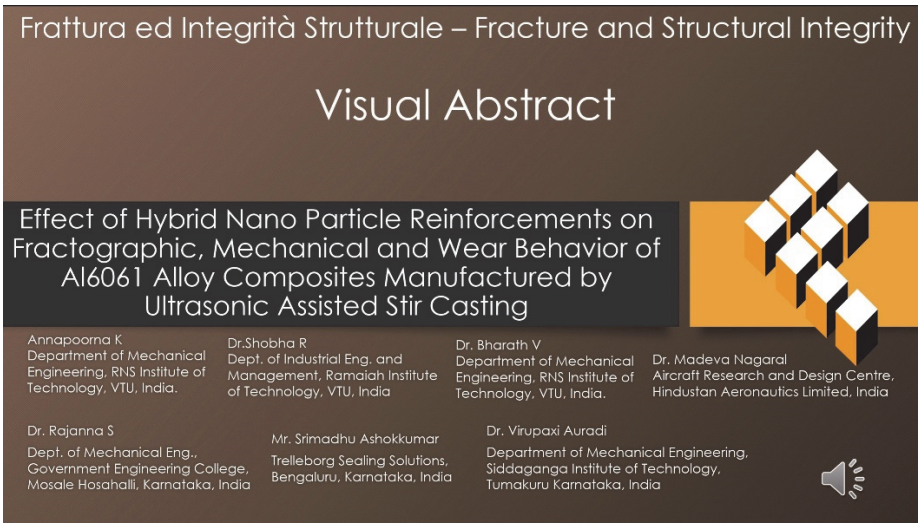

Citation: Annapoorna, K., Shobha, R., Bharath, V., Rajanna, S., Ashokkumar, S., Nagaral, M., Auradi, V., Effect of Hybrid Nano Particle Reinforcements on Fractographic, Mechanical and Wear Behavior of Al6061 Alloy Composites Manufactured by Ultrasonic Assisted Stir Casting Technique, Frattura ed Integrità Strutturale, 71 (2025) 285-301.

Received: 25.09.2024
Accepted: 03.11.2024
Published: 05.12.2024
Issue: 01.2025

KEYWORDS. Al6061 alloy, Nano Al_2O_3 and ZrO_2 Particles, Mechanical and Wear properties, Fractography, Worn Morphology.

INTRODUCTION

Composites are the most promising materials of recent interest because they can fulfill the increasing demands of contemporary technology and surpass the constraints of traditional monolithic materials in achieving good combinations of strength, toughness, and density, among other properties. Ecologically friendly nano- composites present novel economic and technological opportunities for the aerospace, automotive, electronics, and biotechnology industries [1-4]. Hard ceramic particles are introduced into the matrix of MMCs to improve their mechanical characteristics and wear resistance. Discontinuous reinforcement is used to strengthen aluminum MMCs, improving their mechanical and physical properties. Metal matrix composites outperform pure alloys in terms of specific strength, modulus, damping capacity, and wear resistance [5-7]. Therefore, ongoing attempts are made to create novel composites and improve those that already exist in order to obtain the needed qualities for specific applications.

Reason being, its great strength, low weight, and resistance to corrosion, Al6061 is most popular alloy used in a various applications, including defense, automotive, and marine. Aluminum alloys are soft and offer less resistance to wear, which limits their usefulness. When hard ceramic reinforcement particles are added to aluminium and its alloys, they make a matrix composite that is strengthened in places and has almost uniform properties [8]. Zirconia has many unique qualities that make it stand out from other ceramics. It has good mechanical strength because it is very tough, great resistance to crack spreading, good thermal resistance, and low thermal conductivity at high temperatures [9]. International interest in the production of hybrid metal matrix composites (HMMCs) is rising. The combined qualities of its reinforcements are present in HMMCs, which also have better mechanical and tribological qualities. Based on this, it looks like mixing a ZrO_2 matrix with a hard nanostructure material like Al_2O_3 will make a great composite reinforcement and make the composite's mechanical qualities better [10]. Various casting techniques, including squeeze casting, stir casting, spray atomization casting, powder metallurgy, and plasma spraying can be used to create HMMC [11, 12]. One of the common production technique used to fabricate metal matrix composites is stir casting, which is presently used in commercial applications and is considered as a particularly promising approach. Stir casting is a great way to make aluminium alloy metal matrix composites with discontinuous reinforcement because the matrix and reinforcement pieces stick together very well, it's easy to make, and it doesn't cost much [7]. The uneven distribution of the particulate is the main issue with this process due to poor wettability and gravity-regulated segregation. Yong Yang et al. [13] and G.I. Eskin et al. [14] devised a novel technique that integrates the solidification process with ultrasonic cavitation to achieve uniform dispersion and distribution of nanoparticles in aluminium matrix nano composites.

Huda A et al. [15] examined the mechanical and wear characteristics of AA7075 aluminium matrix composites reinforced with Al_2O_3 nanoparticles by incorporating 0, 1, 3, and 5% of Al_2O_3 nanoparticles, concluding Investigating the tribological properties of nano-sized ZrO_2 ceramic particles in automobile lubricants, A D Toth et al.[16] Incorporating ZrO_2 nano ceramic powder as a lubricant additive, a tribometer was used to evaluate the tribological performance of the samples and find an ideal concentration of 0.4 weight percent. The mechanical properties of aluminium alloy reinforced with silicon carbide nanoparticles were explored by Pradeep et al. [17] and they found that incorporation of nanoparticle reinforcement improved compressive strength, yield strength, tensile strength, and hardness.

According to the literature review, various studies have been published on aluminium alloy metal matrix composites with nanoparticle reinforcement; nevertheless, there is a paucity of research on hybrid nanoparticle reinforcement. Current study aims to produce an aluminium metal matrix composite utilizing alumina and zirconia as reinforcements to create a novel material and examine the impact of nano-reinforcement on the mechanical and wear properties of the resultant composite. Stir casting is a widely acknowledged and economically viable technique for the mass production of MMCs. Ultrasonic-assisted stir casting is a technique that enhances matrix particle adhesion, regulates matrix structure, and reduces production costs [19-20]. Aluminum-based composites are regarded as viable substitutes for steel or aluminium alloys in numerous contemporary applications. In this epoch, novel formulations and property assessments are requisite. This study examines the influence of nano hybrid reinforcement on the mechanical and wears properties of Al6061 hybrid metal matrix composites.

EXPERIMENTAL DETAILS

Materials

In the current work, Al6061 aluminium alloy functioned as the matrix and was augmented with nano Al_2O_3 and nano ZrO_2. Supplier Name: Nano Research Lab The raw material was analyzed with Energy Dispersive X-ray Analysis equipment (EDAX) to confirm its chemical makeup. Tab. 1 delineates the constituent composition of the Al6061 alloy, whereas the SEM and EDAX plot reveals peaks corresponding to the base alloy, Al_2O_3, and ZrO_2, as illustrated in Fig. (1-6) respectively.

Material	Density (g/cm^3)	Melting point (°C)	Modulus of Elasticity (GPa)	Brinell Hardness	Poisons Ratio	Tensile Strength(MPa)
Al6061	2.7	585	68.9	30-33	0.33	110-182
Al_2O_3	3.98	2072	370	450-500	0.21	650-660
ZrO_2	5.68	2715	94.5	130-145	0.34	300-330

Table 1: Elemental composition of Al6061 alloy.

Mg	Si	Ti	Cr	Mn	Fe	Cu	Zn	Al
0.81	0.62	0.1	0.13	0.11	0.35	0.2	0.12	Balance

Table 2: Properties of matrix and reinforcement material.

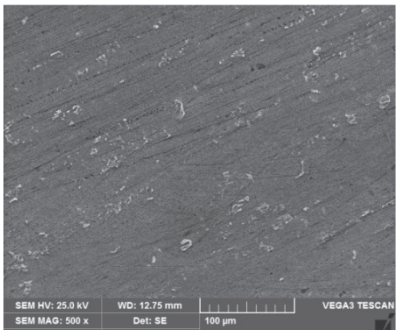

Figure 1: SEM image of Al6061.

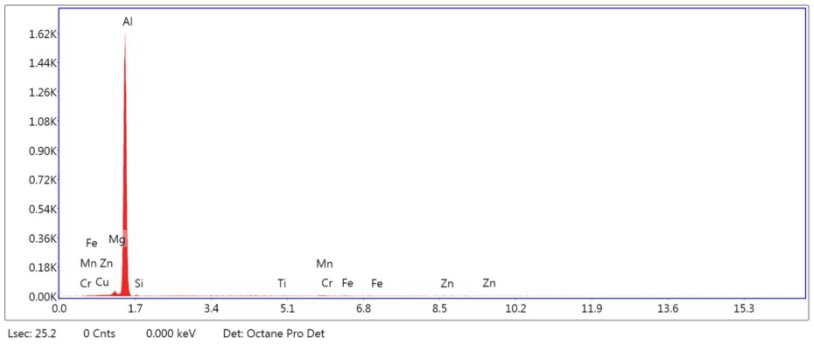

Figure 2: EDS Spectrum of Al6061.

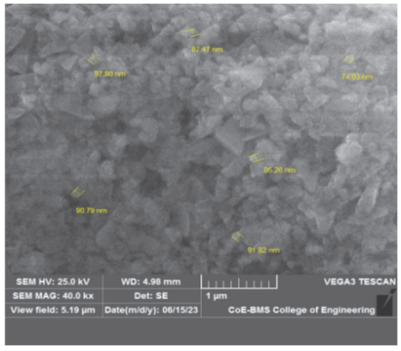

Figure 3: SEM image of Al_2O_3.

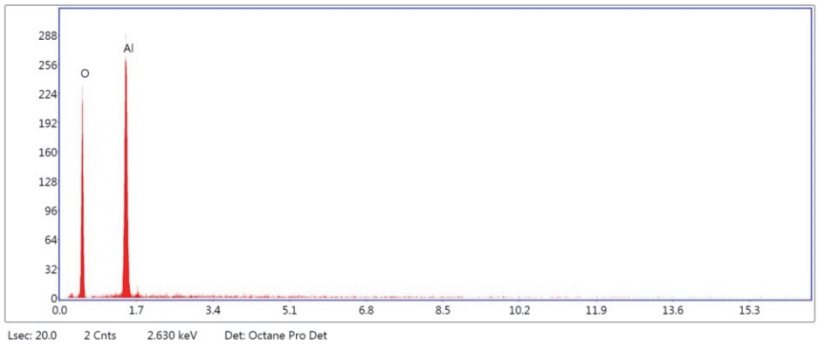

Figure 4: EDS Spectrum of Al_2O_3.

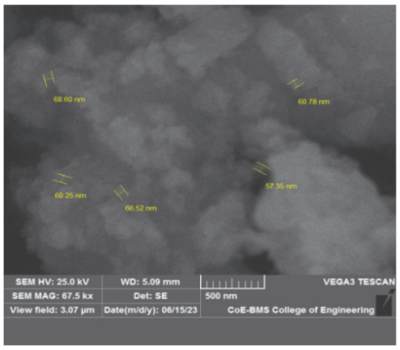

Figure 5: SEM image of ZrO_2.

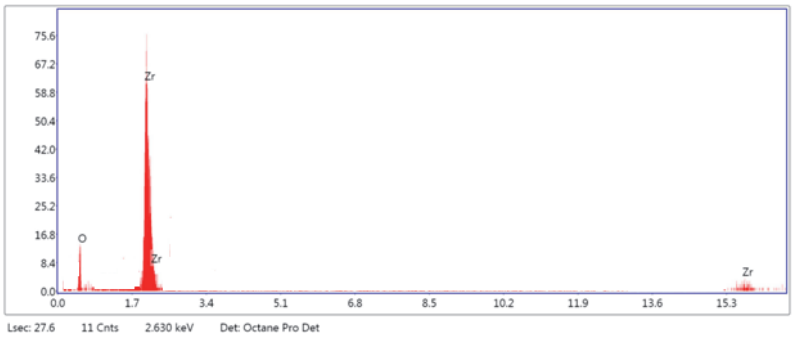

Figure 6: EDS Spectrum of ZrO_2.

Fabrication Procedure:

The proposed hybrid nano composite is produced using Al6061 Alloy having chemical composition as shown in Tab. 1. Nano alumina (n Al_2O_3) and nano zirconia (n-Zro_2) having average particle size of 50-90nm were used as reinforcement. The fabrication of the composite material Al6061/Al_2O_3/ZrO_2 of variable weight percentage (0.5, 0.75, 1 and 1.25 wt% Al_2O_3 and 0.5, 0.75, 1 and 1.25 wt% ZrO_2) was carried out by using ultrasonic assisted stir casting technique.

Fig. 7 shows stir casting experimental setup (make: Swamequip) used in fabricating hybrid MMC. It consists of electrical induction furnace, Crucible, stirring set up, Thermocouples, Weighing scale, Digital timer and an ultrasonic vibrator.

Figure 7: Stir Casting Machine.

Figure 8: Stirring of Molten Metal.

Al6061 ingots were placed inside the induction furnace and melted until it reached the desired molten state at the temperature 750 degree Celsius; once this temperature was attained, solid hexachloroethane was incorporated in the melt for effective degassing. Preheated nano ZrO_2 (0.50, 0.75, 1.00 and 1.25 wt%) and nano Al_2O_3 (0.50, 0.75, 1.00 & 1.25 wt%) particles at 250°C were introduced in the vortex of the liquefied alloy. The reinforcement was preheated to eliminate any moisture and ensure uniform dispersion during stirring. Stirring was done by mechanical means at speed 500 RPM for a stirring time 10 minutes to form a vortex and disperse the nanoparticles in the melt. The combining of nanoparticles is challenging with traditional mechanical rotary impellers due to the high surface area-to-volume ratio of the nanoparticles and the tendency for clustering prior to integration into molten liquid, attributable to the inadequate wetting properties of ultrafine particles with dense liquids. To mitigate this limitation, an ultrasonic-assisted stirring approach is employed to promote the dispersion of ceramic nanoparticles by disrupting agglomerations and submicron clusters, hence improving wettability. This process occurs at a liquidus temperature over 750 °C, which improves the fluidity of the molten liquid and boosts the wettability of nanoparticles to the matrix, as well as the flow ability of the molten metal, with increasing temperature [21]. Following 10 minutes of mechanical stirring, an ultrasonic vibrator (Probe) was employed to disperse the ceramic nanoparticles inside the metal pool for uniform mixing. The probe is positioned at three-quarters of the liquid's depth and permitted to vibrate. These vibrations generate high-energy waves, resulting in numerous cavitation bubbles within the molten pool. The cavitation bubbles exhibit elevated temperature and pressure, which detonate within microseconds due to pressure differentials, fragmenting clusters and uniformly dispersing the agitated nanoparticles throughout the liquid metal. The molten material was thereafter put into the preheated (400°C)

mould to prevent stress concentration, and the cast substance was permitted to cool and solidify within the mould prior to its removal for further examination. SEM was used for the microstructural study of the produced composites; mechanical and wear criteria were also assessed. To minimize errors, three test specimens were evaluated for each test, and the average of the three readings was calculated.

Sample No.	Matrix	Al_2O_3 (%)	ZrO_2 (%)
1	Al6061	0	0
2		1	0.5
3		1	0.75
4		1	1
5		1	1.25
6		0.5	1
7		0.75	1
8		1.25	1

Table 3: Weight percentage of matrix and reinforcement material.

Experimental details

Microstructural investigations were conducted using a scanning electron microscope (Model: Tescan Vega 3) to examine the distribution of reinforcing elements, specifically Al_2O_3 and ZrO_2 particles, within the Al6061 matrix. The device features electron cannon with a tungsten heated cathode, either in discrete stages or continuously, a resolution of 3.0 nm at 30 kV, magnification ranging from 4.5X to 1,000,000X, and a scanning speed changeable from 20ns to 10 ms per pixel.

ASTM standard B311-22 is followed for determining the density of composite. This standard specifies the test methods for determining the density of aluminum and its alloys by the water displacement method. Density is assessed for each sample using a Mettler Toledo specific gravity measurement instrument. First, the weight of the specimen is measured in air, and then the same specimen is measured in water. The density is calculated based on the weight difference between the measurements in air and water.

To acquire test samples in accordance with ASTM requirements, the manufactured hybrid metal matrix composites of Al6061 containing 0.5, 0.75, 1, and 1.25 wt% Al_2O_3 and ZrO_2 were machined utilizing a wire EDM machine. The hardness of the Al6061 composite, reinforced with nano ZrO_2 and nano Al_2O_3, was assessed using a Vickers Hardness Tester (Mitutoyo HM). The test was performed as per ASTM E384-22 standard. The samples were polished to a smooth, reflective gloss to guarantee that surface flaws do not influence the hardness test. A Vickers hardness tester employing a diamond indenter is utilized for the assessment. The load is incrementally introduced to prevent shock and maintained for duration of 10 seconds at a force of 0.5 kgf (kilogram-force).

To examine the potential impact of the indenter on tougher particles, the test was performed at three distinct sites, and the hardness of the samples was ascertained by averaging three separate measurements. Tensile tests conducted in compliance with ASTM E8-22 utilizing an INSTRON-5980 computerized universal testing machine (UTM) with a maximum capacity of 50 kN and a minimum resolution of 1 N had We evaluated the fabricated nano hybrid composite's tensile characteristics—that of yield strength, ultimate tensile strength, and ductility. The SEM examination was utilized to investigate the shattered surfaces, ascertain the fracture mechanism, and conduct microstructural studies. The wear characteristics of the composite were evaluated by wear testing. The engineered composite specimens were subjected to dry sliding wear assessment with a pin-on-disc tribometer. The experiments were performed on cylindrical specimens measuring 10 mm in diameter and 25 mm in height. The ASTM G99-23 standard provided the framework for the wear testing conducted in this investigation. An EN-32 steel disc with an 80 mm track diameter served as the counter-face for specimen testing. This study examined the wear behaviour of the composites under various situations. The wear test was conducted by altering load, distance and velocity of sliding. Fractured specimens and abraded regions were examined using SEM to analyze wear and fracture.

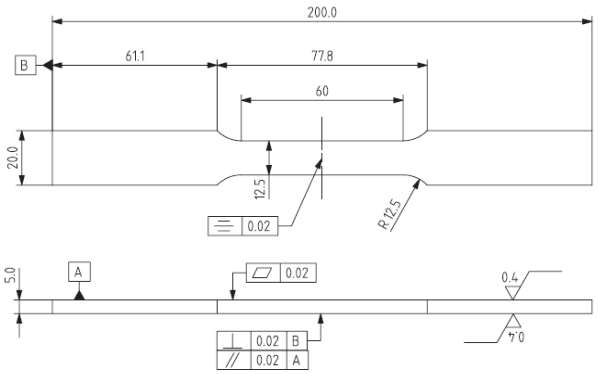

Figure 9: Tensile specimen specification.

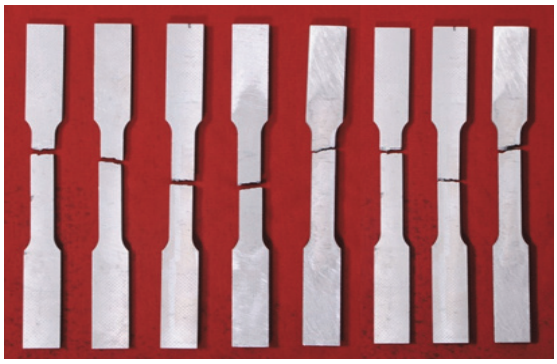

Figure 10: Tensile specimens.

Figure 11: Pin on disc wear tester.

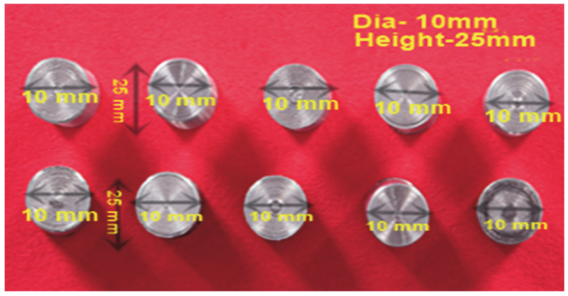

Figure 12: Wear specimens.

RESULTS AND DISCUSSION

Micro structural characterization of Al6061/Al_2O_3/ZrO_2 hybrid nano composite with different weight fractions

The microstructure of the SEM image of Al6061-1% Al_2O_3-0.5% ZrO_2, Al6061-1% Al_2O_3-1.25% ZrO_2, and Al6061-1.25% Al_2O_3-1% ZrO_2 depicted in Fig. 14 (a-c). EDS proved that the sample's real chemical makeup was present in certain areas. Fig. 13 shows the energy dispersive spectroscopy results for Al6061 that has been strengthened with 1% Al_2O_3 and 1% ZrO_2. These results show that the reinforcements are present in the aluminium matrix. The stir casting process makes mixtures of Al6061, Al_2O_3, and ZrO_2. The prepared composite had this even spread out texture because it was made with an ultrasonic-assisted stir casting method. When the stirring time (10 minutes) and speed (500rpm) are just right, the particles are spread out more evenly and the matrix and reinforcement stick together well. Fig. 14(b, c) shows areas of clustering and agglomeration, which is probably because there is a lot of reinforcing. As the weight percentage of reinforcement increases, the link between the soft matrix and hard ceramic reinforcement particles weakens. This causes the surface energy to rise, therefore influencing the clustering [23]. The 1% Al_2O_3 and 1% ZrO_2 particles were spread out more evenly, as shown by SEM studies of the microstructures. Higher filled composites, on the other hand, showed that these particles separated and clumped together. This separation probably happens when solidifies, since dendrites form first. This lets extra particles move and group together in the spaces between the dendrites at the solid-liquid contact. Sample had 1% Al_2O_3 and 1.25% ZrO_2, so the separation was more noticeable. The combination with 1% Al_2O_3 and 1% ZrO_2 has strong bonds between the reinforcing ceramic particles and the Al6061 matrix, which means that load, is transferred efficiently and the structure is more stable. It's clear that the production process worked well because there are no major flaws like holes, cracks or particle agglomeration.

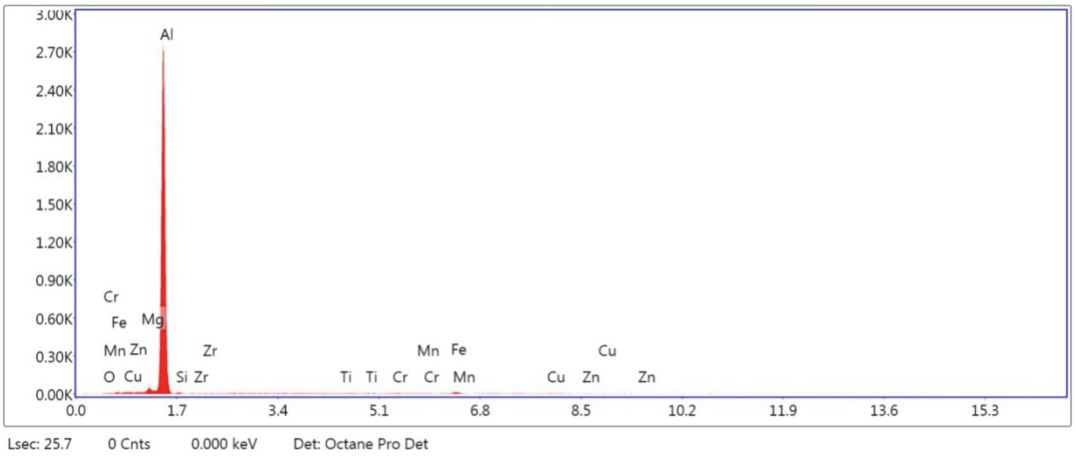

Figure 13: EDS spectrum and SEM image of Al6061-1% Al_2O_3-1%ZrO_2.

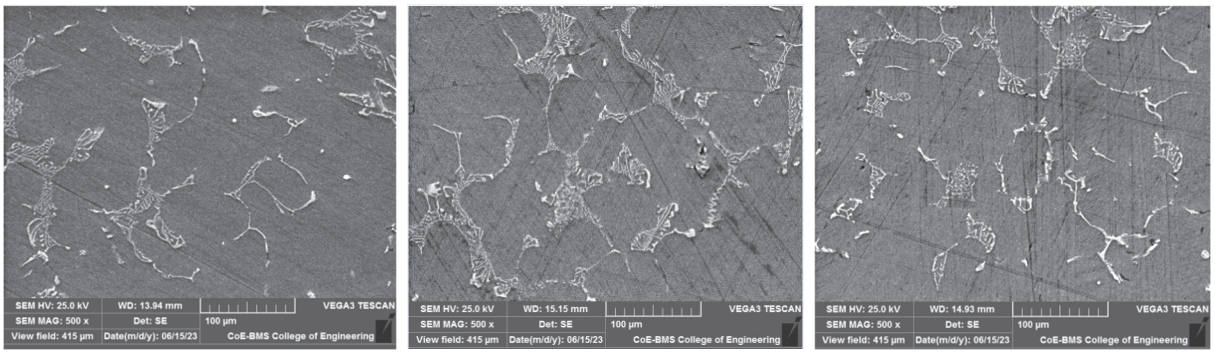

14(a) 14(b) 14 (c)

Figure 14: (a) SEM image of Al6061-1% Al_2O_3-0.5% ZrO_2, (b) SEM image of Al6061-1% Al_2O_3-1.25% ZrO_2, (c) SEM image of Al6061-1.25% Al_2O_3-1% ZrO_2.

Sample No.	Composition	Theoretical Density(g/cm^3)	Experimental Density (g/cm^3)
1	Al6061	2.700	2.693
2	Al6061-1%Al_2O_3-0.5%ZrO_2	2.728	2.721
3	Al6061-1%Al2O_3-0.75%ZrO_2	2.736	2.732
4	Al6061-1%Al_2O_3-1%ZrO_2	2.744	2.739
5	Al6061-1%Al_2O_3-1.25%ZrO_2	2.752	2.75
6	Al6061-0.5%Al_2O_3-1%ZrO_2	2.738	2.734
7	Al6061-0.75%Al_2O_3-1 %ZrO_2	2.741	2.739
8	Al6061-1.25%Al_2O_3-1%ZrO_2	2.748	2.743

Table 4: Theoretical and Experimental density of prepared composites.

Density

Tab. 4 and Fig. 15 shows the theoretical and experimental densities of Al6061 alloys that have been strengthened with different amounts of nano Al_2O_3 and nano ZrO_2 particles. When nano reinforced ZrO_2 and Al_2O_3 are added to Al6061, the total density of the composite material goes up in a noticeable way. Theoretical density was found using the rule of mixing. The actual densities are very close to the theoretical densities. This suggests that the methods used in the

experiments were correct and reliable. The samples are likely to be homogeneous since the measured and estimated densities are very close to each other. This means that ZrO_2 and Al_2O_3 were evenly spread out in the aluminium matrix, which is important for making sure that the material's qualities are the same all over. The actual density is sometimes lower than the theoretical density. This might be because of the pores that form during the manufacturing process. Porosity could be caused by the gas getting trapped during casting, the movement of hydrogen, or the material shrinking as it hardens [24]. Hence, the addition of nano Al_2O_3 and nano ZrO_2 particles to Al6061 alloy resulted in increased density, indicating a homogeneous distribution of nanoparticles.

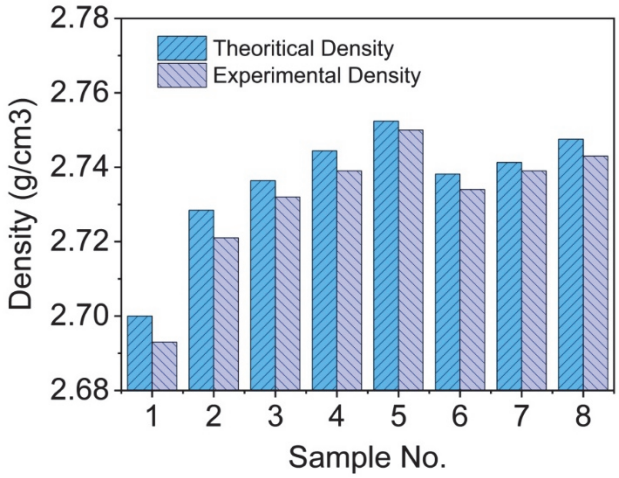

Figure 15: Density of Al6061 alloy: Theoretical and Experimental comparison by varying compositions of nano Al_2O_3 and ZrO_2 reinforcement

Hardness test

A Vickers Hardness Tester (Mitutoyo HM) was used to check the hardness of a metal called Al6061 that had different amounts of Al_2O_3 and ZrO_2 nanoparticles added to it (0.5, 0.75, 1, and 1.25 wt. %). Tab. 5 shows the effects of different compositions on hardness, and Fig. 16 shows a graph of those effects. It is clear that the mixture gets harder as the amounts of ZrO_2 and Al_2O_3 in it go up. Pure aluminium has a hardness of 60.8 Hv, which is not very high because it is soft and easy to shape. The incorporation of nano Al_2O_3 and nano ZrO_2 particles significantly improved the hardness of Al6061 alloy, with a maximum hardness of 90.9 Hv achieved at 1% ZrO_2 and 1.25% Al_2O_3. Hence, increase in wt. % of nano reinforced particulates enhances the hardness of the produced composites. Similar trends were observed [7]. Also, there are hard ceramic nanoparticles called ZrO_2 and Al_2O_3 in the aluminium alloy core. These particles stop dislocations from moving, which makes the material harder. The second reason is that the ZrO_2 and Al_2O_3 nanoparticles have a big stabilizing effect on the movement of grain boundaries. This makes the grains more uniform and strengthens the grain boundaries, which makes the material harder.

Sample No.	Composition	Hardness, Hv
1	Al6061	60.8
2	Al6061-1% Al_2O_3-0.5%ZrO_2	77.2
3	Al6061-1% Al_2O_3-0.75% ZrO_2	84.8
4	Al6061-1% Al_2O_3-1% ZrO_2	88.2
5	Al6061-1% Al_2O_3-1.25% ZrO_2	89.3
6	Al6061-0.5% Al_2O_3-1% ZrO_2	75.1
7	Al6061-0.75% $Al_2O_3$1 % ZrO_2	82.6
8	Al6061-1.25% Al_2O_3-1% ZrO_2	90.9

Table 5: Vickers Hardness of Al6061 Alloy with different wt% of nano Al_2O_3 and nano ZrO_2 reinforcements.

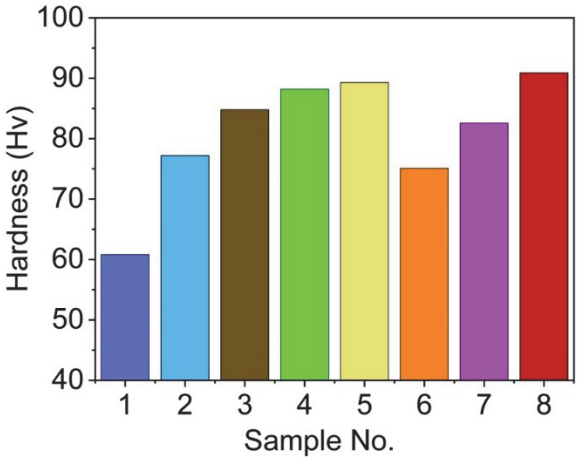

Figure 16: Vickers hardness of Al6061 alloy with different wt% of Al_2O_3 and ZrO_2 reinforcements

Tensile test

Tensile tests were used to evaluate elongation, Young's Modulus (YM), Ultimate Tensile Strength (UTS), and Yield Strength (YS). Tab. 6 summarizes the tensile parameters of aluminium composites with varying weight percentages of nano zirconium dioxide (ZrO_2) and nano aluminium oxide (Al_2O_3). The investigation underscores the influence of additives on the mechanical properties of composite materials. Pure aluminium demonstrates inferior mechanical capabilities coupled with considerable elongation, signifying excellent ductility. Augmenting the concentrations of ZrO_2 and Al_2O_3 has improved the YM, YS, and UTS of aluminium composites. Sample 3, which contained 1 wt. % of ZrO_2 and 1 wt. % of Al_2O_3 nanoparticles as reinforcement, exhibited the highest Young's modulus (70.8 MPa), yield strength (120.5 MPa), and ultimate tensile strength (194.8 MPa), demonstrating an optimal synergy of these additives for enhanced strength while preserving adequate ductility. The percentage of elongation constantly diminishes with the incorporation of ZrO_2 and Al_2O_3. Pure aluminium has the greatest ductility (14.20%), which markedly diminishes with the increased ceramic content in sample 7 containing 1% ZrO_2 and 1.25% Al_2O_3, signifying a compromise between strength and ductility.

The enhancements in mechanical properties may stem from a low degree of porosity and uniform distribution of nanoparticles. The integration of nanoparticles into the matrix offers limited heterogeneous nucleation sites during solidification, leading to refined grains, which enhances the tensile strength of the nano composite. The addition of nano Al_2O_3 and nano ZrO_2 has enhanced grain boundary integrity by refining the grain structure, leading to improved yield and tensile strengths. The thermal mismatch between the aluminium matrix (23 x 10^-6/°C) and the ceramic ZrO_2 particles (10.5 x 10^-6/°C) and Al2O3 particles (8.2 x 10^-6/°C) results in an increase in dislocation density, independent of the entrapment of dislocations in the matrix by the second phase ceramic Al_2O_3 and ZrO_2 particles during deformation [22, 25]. Figs. 17, 18, 19, and 20 indicate that the composite Al6061 reinforced with 1% ZrO_2 and 1% Al_2O_3 (Sample 3) exhibits the greatest balanced improvement in mechanical properties, surpassing those of the as-cast 6061 Al alloy.

Sample no.	Al_2O_3 (%)	ZrO_2 (%)	YM (MPa)	YS (MPa)	UTS (MPa)	Elongation (%)
1	0	0	68.2	81.6	144.52	14.20
2	1	0.5	68.7	104.8	171.53	5.33
3	1	0.75	69.3	110.3	180.90	4.75
4	1	1	70.8	120.5	194.8	4.6
5	1	1.25	70.1	117.8	189.8	4.15
6	0.5	1	69.1	108.2	177.65	5.46
7	0.75	1	69.6	112.9	183.90	5.05
8	1.25	1	69.8	115.2	185.9	3.95

Table 6: Tensile characteristics of Al6061 alloy with various wt% of Al_2O_3 and ZrO_2 reinforcements.

Fig. 20 displays the percentage elongation for produced composites, which indicates that as particle content increases, the elongation decreases, similar trends were seen [11]. The reason for decrease in elongation is the lower flexibility of the ceramic reinforcement with the matrix. The unshaped ZrO_2 and Al_2O_3 particles may induce localized pressure around them, and over time, the accumulation of particles near the grain boundaries intensifies this pressure concentration. Overall, the addition of nano Al_2O_3 and nano ZrO_2 particles enhanced the tensile properties of Al6061 alloy, with optimal results obtained at 1% ZrO_2 and 1% Al_2O_3, demonstrating a balanced improvement in strength and ductility.

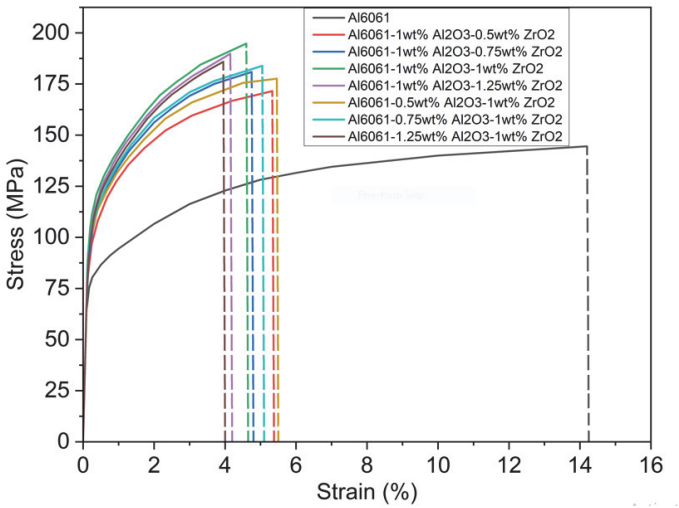

Figure 17: Stress-Strain curves for Al6061 alloy with various wt% of Al_2O_3 and ZrO_2 reinforcements

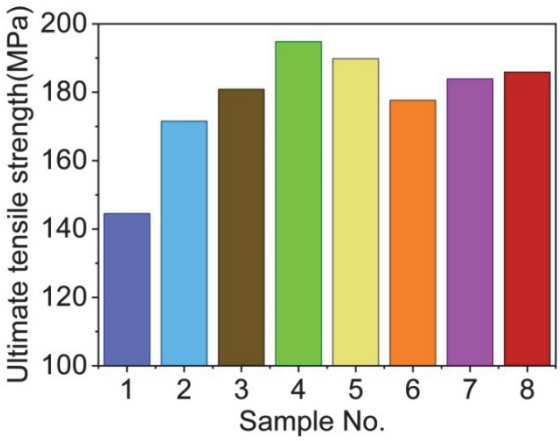

Figure 18: YS of Al6061 alloy and its reinforced composites.

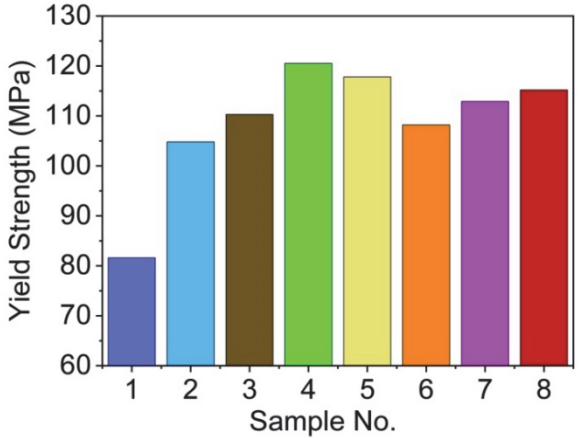

Figure 19: UTS of Al6061 alloy and it's reinforced composites.

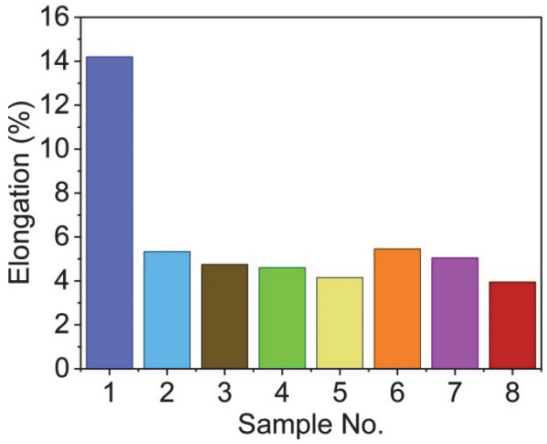

Figure 20: Elongation of Al6061 alloy and its reinforced composite.

Fractography

A critical step in understanding material failure involves examining the fractured surfaces of alloys and their composites. Fig. 21 (a-f) displays the fractured surfaces of the fabricated composites with different weight fractions of reinforcement. The base matrix, Fig. 21(a) exhibited a smooth and consistent surface with shallow, evenly distributed depressions, indicating a fracture that stretches without breaking. In contrast, the composite material showed depressions oriented in two directions. Larger depressions absorbed the reinforcing particles, while smaller depressions were due to the breakdown of the stretchable matrix. SEM analysis of the damaged composite surfaces (Figs. 21(b-d)) revealed fine cracks in the n-Al_2O_3 and n-ZrO_2 particles, partial separation between the matrix and reinforcement, and even matrix fracture. Generally, the fracture surfaces displayed smooth particles, indicating particle fracture rather than separation, which suggests strong interfacial bonds in these composites.

The Al6061 matrix composites with elevated filler content (Fig. 21(e) and (f)) exhibited both large and tiny dimples, indicating that the failure mechanism was attributable to the growth, coalescence, and eventual rupture of ductile voids. The incorporation of n-Al_2O_3 and n-ZrO_2 modified the fracture characteristics of the Al6061 matrix, transitioning from ductile to brittle modes, and subsequently to a hybrid ductile mode. The n-Al_2O_3 and n-ZrO_2 particles had minor dimples alongside the matrix and hairline fractures. Fractography studies demonstrate a significant correlation between reinforcement and the matrix, resulting in improved mechanical properties of hybrid nano composites. Consequently, the results of UTS, YS, and % elongation can be correlated with fractographic analyses and are suitably relevant.

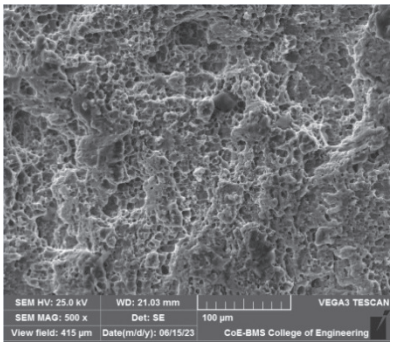

21(a)

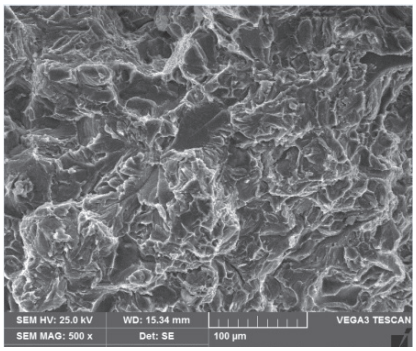

21(b)

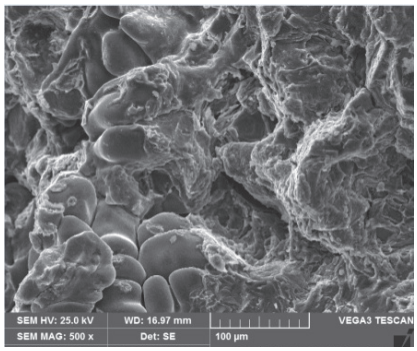

21(c)

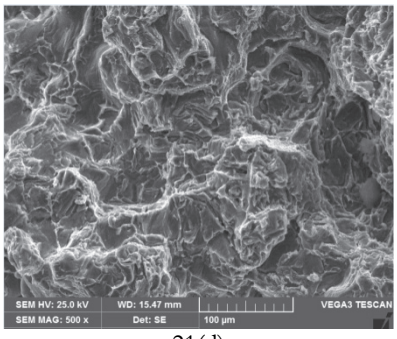

21(d)

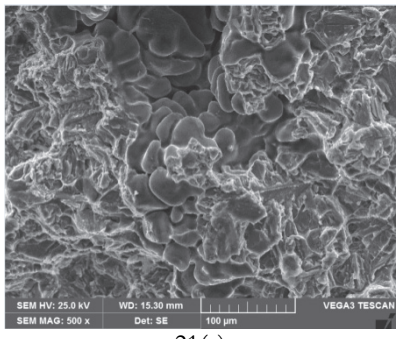

21(e)

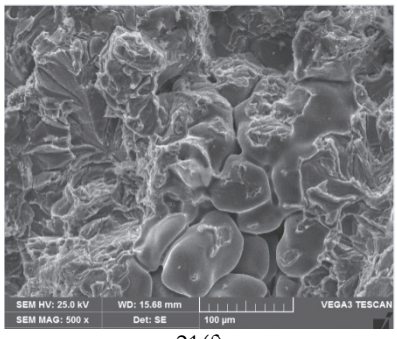

21(f)

Figure 21(a-f): Fractography of images of (a) Al6061, (b) Al6061-1% Al_2O_3-0.5% ZrO_2, (c) Al6061-1% Al_2O_3-0.75% ZrO_2, (d) Al6061-1% Al_2O_3-1% ZrO_2, (e) Al6061-1% Al_2O_3-1.25% ZrO_2, (f) Al6061-1.25% Al_2O_3-1% ZrO_2.

Wear Characteristics - Effect of load

The wear tests were performed by altering load, speed, and sliding distance. Tab. 7 presents the exact wear rate values as a function of changing load, while maintaining constant speed and sliding distance. Loads of 10 N, 20 N, 30 N, and 40 N were applied at a speed of 4 m/s across a distance of 4000 meters, and the results were recorded. Fig. 22 illustrates the wear rate in relation to different loads at ambient temperature. The wear rate was shown to grow progressively with the elevation of load. The highest wear rate is noted in the as-cast Al6061 alloy. Al6061 reinforced with 1 wt. % Al_2O_3 and 1 wt. % ZrO_2 exhibited the lowest wear rates, indicating its exceptional wear resistance. The enhancement in wear resistance can be ascribed to the substantial adhesive metal-metal contact that facilitated surface shear strain [26].

Load (N)	Specific wear rate (x 10-4)							
	As Cast Al6061	Al6061-1wt% Al_2O_3-0.5wt% ZrO_2	Al6061-1wt% Al_2O_3-0.75wt% ZrO_2	Al6061-1wt% Al_2O_3-1wt% ZrO2	Al6061-1wt% Al_2O_3-1.25wt% ZrO_2	Al6061-0.5wt% Al_2O_3-1wt% ZrO_2	Al6061-0.75wt% Al_2O_3-1wt% ZrO_2	Al6061-1.25wt% Al_2O_3-1wt% ZrO_2
10	4.58	3.62	3.08	2.40	2.56	4.02	3.36	2.75
20	5.64	4.45	3.86	2.85	3.25	4.95	3.99	3.52
30	6.45	5.25	4.37	3.45	3.80	5.89	4.80	4.06
40	7.70	6.17	5.06	4.01	4.39	6.89	5.72	4.62

Table 7: Produced Composites specific wear rate at 4.0 m/sec as a sliding velocity , 4000m as a sliding distance with varying load.

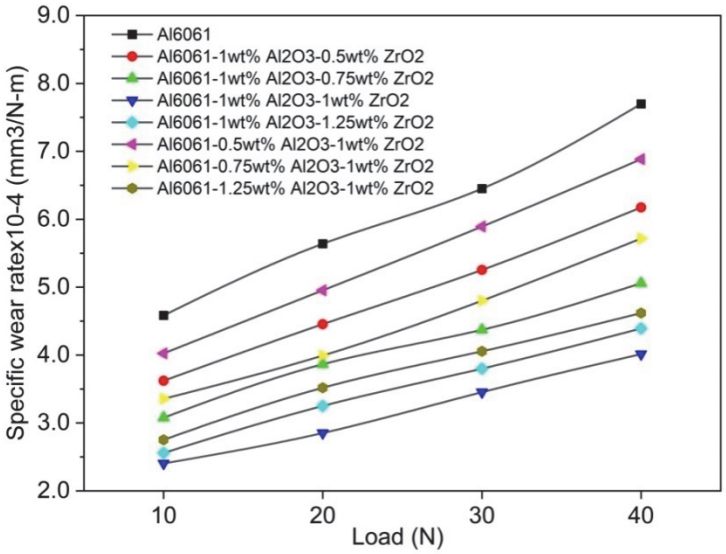

Figure 22: Specific wear rate of composites under different loads at 4.0m/s and 4000m distance

Velocity (m/s)	Specific wear rate, (x 10-4)							
	As Cast Al6061	Al6061-1wt% Al_2O_3-0.5wt% ZrO_2	Al6061-1wt% Al_2O_3-0.75wt %ZrO_2	Al6061-1wt% Al_2O_3-1wt% ZrO_2	Al6061-1wt% Al_2O_3-1.25wt% ZrO_2	Al6061-0.5wt% Al_2O_3-1wt% ZrO_2	Al6061-0.75wt% Al_2O_3-1wt% ZrO_2	Al6061-1.25wt% Al_2O_3-1wt% ZrO_2
1	5.09	3.94	3.37	2.60	2.79	4.55	3.63	3.00
2	5.96	4.64	3.96	3.11	3.36	5.30	4.33	3.62
3	6.92	5.38	4.61	3.65	3.83	6.22	5.00	4.09
4	7.70	6.17	5.06	4.01	4.39	6.89	5.72	4.62

Table 8: Produced Composites specific wear rate at 40N as a load, 4000m as a sliding distance with varying sliding velocity.

Wear Characteristics - Effect of variable speed

Tab. 8 presents the exact wear rate values as a function of varying speed, while maintaining constant load and sliding distance. In this experiment, velocities were adjusted to 1 m/s, 2 m/s, 3 m/s, and 4 m/s, while maintaining a constant weight of 40 N and a sliding distance of 4000 meters. Fig. 23 illustrates the correlation between wear rate and varying speeds. The figure illustrates that an increase in speed results in a higher wear rate. As velocity escalates, the resultant frictional heat elevates the surface temperature, subsequently causing material softening, which exacerbates damage and further amplifies the wear rate. The maximum wear rate is seen in the as-cast Al6061 alloy. Al6061 reinforced with 1 wt.

% Al_2O_3 and 1 wt. % ZrO_2 exhibited the lowest wear rates, likely due to the creation of intermetallic particles that are uniformly aligned, hence augmenting the strength of the aluminium alloy matrix.

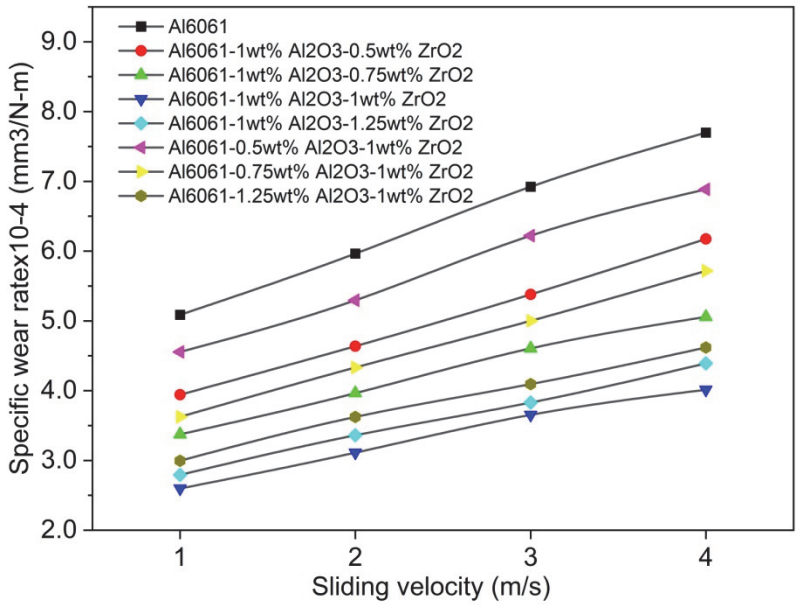

Figure 23: Specific wear rate of composites under different velocities at 40N and 4000m distance

Wear Characteristics - Effect of variable sliding distance

Further, keeping a constant load of 40 N and speed of 4 m/s and varying the sliding distances by 1000, 2000, 3000, and 4000 meters the wear rate of the samples were tested and the results were tabulated in Tab. 9. Fig. 24 indicates that an increase in sliding distance correlates with a rise in wear rate. Abrasion occurs between sliding surfaces, resulting in material bluntness and an expanded contact area, which may contribute to heightened wear behaviour. Additionally, as the sliding distance increases, plastic deformation in the subsurface region leads to the disintegration of the tribo layer, thereby elevating the wear rate.

The specimen with 1 wt. % Al_2O_3- 1 wt. % ZrO_2 had the lowest specific wear rate at all test circumstances, suggesting better wear resistance over Al6061. However, the hybrid nano composite with 1 wt. % Al_2O_3- 1.25 wt % ZrO_2 showed an increase in wear rate at higher loads, suggesting a complex interplay between nanoparticle content and load conditions. The results imply that although ceramic reinforcements might improve wear resistance, suitable nanoparticle concentrations have to be carefully taken into account to maximize performance under particular operational environments.

Distance (m)	Specific wear rate, (x 10-4)							
	As Cast Al6061	Al6061-1wt% Al_2O_3-0.5wt% ZrO_2	Al6061-1wt% Al_2O_3-0.75wt% ZrO_2	Al6061-1wt% Al_2O_3-1wt% ZrO_2	Al6061-1wt% Al_2O_3-1.25wt% ZrO_2	Al6061-0.5wt% Al_2O_3-1wt% ZrO_2	Al6061-0.75wt% Al_2O_3-1wt% ZrO_2	Al6061-1.25wt% Al_2O_3-1wt% ZrO_2
1000	6.40	5.19	4.22	3.25	3.71	5.68	4.85	3.88
2000	6.74	5.53	4.50	3.56	3.87	6.08	5.17	4.18
3000	7.25	5.87	4.87	3.85	4.14	6.62	5.40	4.35
4000	7.70	6.17	5.06	4.01	4.39	6.89	5.72	4.62

Table 9: Produced composites specific wear rate at 40N as a load, 4.0 m/s as a sliding distance with varying sliding distance.

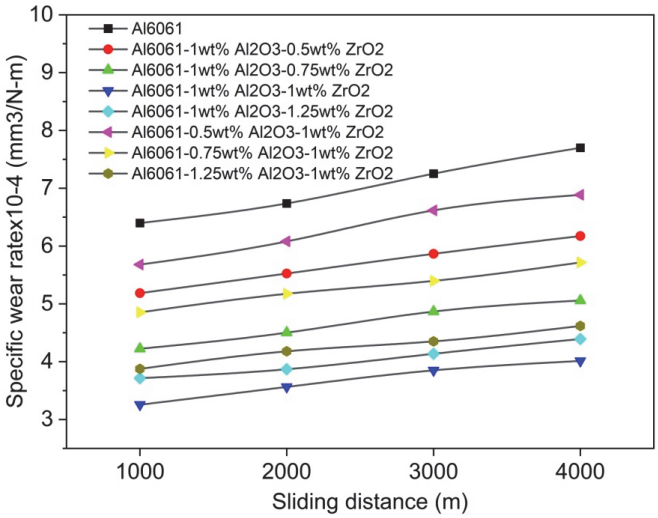

Figure 24: Specific wear rate of composites under different sliding distances at 40N and 4.0 m/s sliding speed.

Overall, the incorporation of nano Al_2O_3 and nano ZrO_2 particles significantly improved the wear resistance of Al6061 alloy, with the lowest wear rate observed at 1% Al_2O_3 and 1% ZrO_2. The wear rate of Al6061 alloy increased with increasing load, speed, and sliding distance, with the hybrid nano composite exhibiting better wear resistance under various test conditions.

Morphology of worn surface

The results of the influence of higher loads, distance and speed on the as cast Al6061 alloy and Al6061 reinforced with varying weight fractions of Al_2O_3 and ZrO_2 nano composites, reveal that Al6061-1 wt. % Al_2O_3- 1 wt. % ZrO_2 are more effective and offer better wear resistance, as compared to other combinations of reinforcement and also to as cast aluminum alloy. In this section the analysis of worn surface is done to understand the mechanism of wear in the fabricated hybrid nano composites.

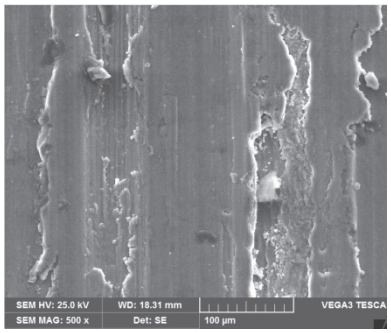

25(a)

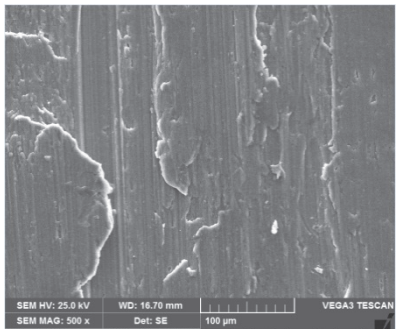

25(b)

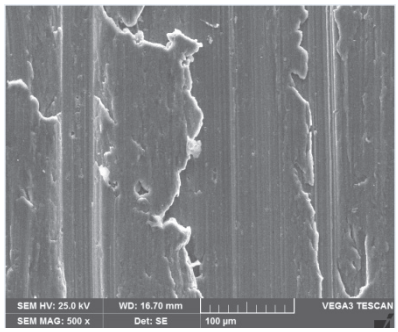

25(c)

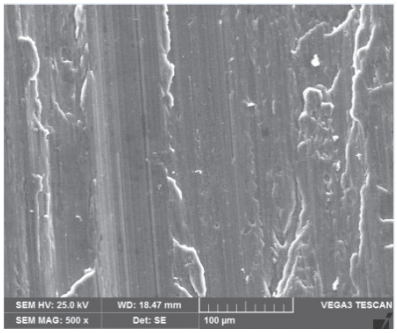

25(d)

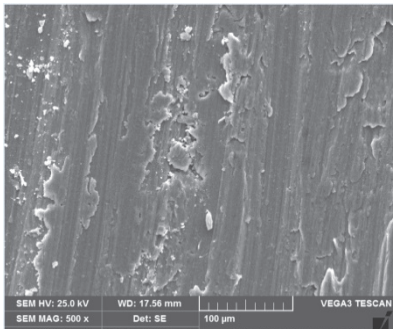

25(e)

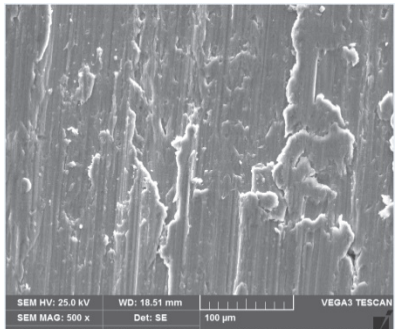

25(f)

Figure 25 (a-f): SEM images of (a) Al6061, (b) Al6061-1% Al_2O_3-0.5% ZrO_2, (c) Al6061-1% Al_2O_3-0.75% ZrO_2, (d) Al6061-1% Al_2O_3-1% ZrO_2, (e) Al6061-1% Al_2O_3-1.25% ZrO_2, (f) Al6061-1.25% Al_2O_3-1% ZrO_2

Fig. 25(a-f) presents the SEM images of the worn surfaces of the as-cast Al6061 alloy and the fabricated composites. The photographs illustrate a distinct contrast between the surface morphology of the worn composites and the as-cast matrix alloy (Fig. 25a). The as-cast Al6061 matrix alloy demonstrates significant plastic deformation on the contact surface, while this phenomenon is scarcely seen in other composites. The Al6061 alloy matrix (Fig. 25a) exhibits large and deep grooves on its surface, characterized by significant thickness and width, while finer grooves are present in other samples (Fig. 25.b, c, e, f). This morphology is absent in the composite containing 1 wt. % Al_2O_3 and 1 wt. % ZrO_2 (Fig. 25.d), suggesting it possesses superior load-bearing capacity during wear testing.

SEM images of Al6061 with 1 wt. % Al_2O_3 and 1 wt. % ZrO_2 (Fig. 25 d) demonstrates that composite experiences minimal damage compared to the as-cast Al6061 matrix alloy and other composites. This is likely because the matrix alloy has less surface strength in comparison to the produced composite and softens more quickly as a result of heat generated at the interface. SEM images (Fig. 25 d) also show that the produced composite consistently results in smooth and thin surfaces under all testing conditions, unlike the Al6061 alloy matrix and the other composites (Fig. 25 a, b, c, e, f) The composite with 1% Al_2O_3 and 1% ZrO_2 exhibits superior wear resistance in contrast to the as-cast alloy and other composites, as clearly seen in the SEM images of the worn surfaces.

Conclusions

Aluminium alloys reinforced with nanoparticles are predominantly employed in the aerospace and automotive industries. The mechanical qualities, such as hardness and tensile strength, of aluminium alloy can be enhanced by using ceramic elements as reinforcement. This study aims to elucidate the differences in attributes resulting from the incorporation of hybrid reinforcement, leading to the following results.

1. Hybrid Composite of Aluminum 6061 alloy using nano Al_2O_3 and ZrO_2 particles as reinforcement were successfully produced with 0.5, 0.75, 1 and 1.25 wt% of Al_2O_3 and 0.5, 0.75, 1 and 1.25 wt% of ZrO2 by utilizing ultrasonic assisted stir casting technique.
2. Microstructural analyses demonstrated a uniform distribution of Al2O3 and ZrO_2 nanoparticles inside the Al matrix. These particles enhanced the microstructure of the cast materials. Among all the fabricated composites, Al6061 reinforced with 1 wt. % Al_2O_3 and 1 wt. % ZrO_2 exhibits a more uniform distribution of particles within the base alloy compared to other reinforcement compositions.
3. Nano composites produced with 1 wt. % Al_2O_3 and 1wt. % ZrO_2 have shown improved results in UTS and YS than the base alloy and other compositions.
4. Al6061 reinforced with 1.25 wt% Al_2O_3 and 1 wt. % ZrO_2 composites exhibit lower percentage of elongation in contrast to the composites with varying weight percentages (0.5, 0.75, 1 and 1.25 wt %) of Al_2O_3 and ZrO_2, as well as cast Al6061 alloy (14.20%)
5. Maximum hardness was detected for the composites with Al6061 matrix reinforced with 1.25 wt% Al_2O_3 and 1 wt%ZrO_2.
6. Composites fabricated with Al6061 including 1 wt. % Al_2O_3 and 1 wt. % ZrO_2 demonstrate a reduced specific wear rate compared to the Al6061 alloy and alternative compositions. The wear rate of nano composites is dependent upon sliding velocity, applied force, and sliding distance.
7. Fractography examination of tensile specimen fractures by SEM demonstrates distinct fracture mechanisms for Al6061 alloy and its Al_2O_3/ZrO_2 reinforced composites at varying weight percentages. The Al6061 alloy exhibits uniform and enlarged dimples, signifying a ductile fracture. The composites reinforced with Al_2O_3 and ZrO_2 exhibit intermediate ductile cracks, characterized by dimples surrounding the reinforcements resulting from the presence of alumina particles.
8. The analysis of the worn out surface reveals that abrasion, delamination, and a synergy of abrasion and adhesion are the predominant wear mechanisms involved in material removal during sliding.

References

[1] Din, S. H., Shah, M. A., Sheikh, N. A. (2019). Nano-composites and their applications: A review Characterization and application of Nanomaterials, 2, DOI: 10.24294/can.v2i1.875.

[2] Kumar, A. P., Aadithya, S., Dhilepan, K. and Nikhil, N. (2016). Influence of nano reinforced particles on the mechanical properties of aluminium hybrid metal matrix composite fabricated by ultrasonic assisted stir casting. ARPN J. Eng. Appl. Sci, 11(2), pp. 1204-1210.
[3] Dahmane, M., Benadouda, M., Bennai, R., Saimi, A., and Atmane, H. A. (2024). Effect of crack on the dynamic response of bidirectional porous functionally graded beams on an elastic foundation based on finite element method. Acta Mechanica, 235(6), pp. 3849-3860. DOI: 10.1007/s00707-024-03906-1.
[4] Mellal, F., Bennai, R., Avcar, M., Nebab, M. and Atmane, H. A. (2023). On the vibration and buckling behaviors of porous FG beams resting on variable elastic foundation utilizing higher-order shear deformation theory. Acta Mechanica, 234(9), pp. 3955-3977. DOI: 10.1007/s00707-023-03603-5.
[5] Amara, R., Riadh, B., Hassen, A. A., Mokhtar, N. and Hadji, L. (2024). Hygrothermal effect of bio-inspired helicoid laminate plate for strengthening damaged RC beam. Mechanics of Advanced Materials and Structures, pp. 1-18. DOI: 10.1080/15376494.2024.2392623.
[6] Murthy, B. V., Auradi, V., Nagaral, M., Vatnalmath, M., Namdev, N., Anjinappa, C., & Qamar, M. O. (2023). Al2014–alumina aerospace composites: particle size impacts on microstructure, mechanical, fractography, and wear characteristics. ACS omega, 8(14), pp. 13444-13455.
[7] Sajjadi, S. A., Ezatpour, H. R. and Beygi, H. (2011). Microstructure and mechanical properties of Al–Al_2O_3 micro and nano composites fabricated by stir casting. Materials Science and Engineering: A, 528(29-30), pp. 8765-8771.
[8] Ghazi, J. H. (2013). Influence of ceramic particles reinforcement on some mechanical properties of AA 6061 aluminium alloy. Engineering and Technology Journal, 31(14 Part (A) Engineering).
[9] Wang, H., Xu, P., Zhong, W., Shen, L. and Du, Q. (2005). Transparent poly (methyl methacrylate)/silica/zirconia nanocomposites with excellent thermal stabilities. Polymer Degradation and Stability, 87(2), pp. 319-327.
[10] Belekar, R. M., Sawadh, P. S. and Mahadule, R. K. (2014). Synthesis and structural properties of Al2O3-ZrO2 nano composite prepared via solution combustion synthesis. Int. J. Res. Eng. Technol., 2, pp. 145-152.
[11] Al-Salihi, H. A. and Judran, H. K. (2020). Effect of Al_2O_3 reinforcement nanoparticles on the tribological behaviour and mechanical properties of Al6061 alloy. AIMS Mater. Sci, 7, pp. 486-498.
[12] Shuvho, M. B. A., Chowdhury, M. A., Hossain, N., Roy, B. K., Kowser, M. A. and Islam, A. (2020). Tribological study of Al-6063-based metal matrix embedded with SiC–Al_2O_3–TiO_2 particles. SN Applied Sciences, 2, pp. 1-14.
[13] Yang, Y., Lan, J. and Li, X. (2004). Study on bulk aluminum matrix nano-composite fabricated by ultrasonic dispersion of nano-sized SiC particles in molten aluminum alloy. Materials Science and Engineering: A, 380(1-2), pp. 378-383.
[14] Eskin, G. and Eskin, D. G. (2003). Production of natural and synthesized aluminum-based composite materials with the aid of ultrasonic (cavitation) treatment of the melt. Ultrasonics sonochemistry, 10(4-5), pp. 297-301.
[15] Al-Salihi, H. A., Mahmood, A. A. and Alalkawi, H. J. (2019). Mechanical and wear behavior of AA7075 aluminum matrix composites reinforced by Al_2O_3 nanoparticles. Nanocomposites, 5(3), pp. 67-73.
[16] Tóth, Á. D., Szabó, Á. I. and Kuti, R. (2021). Tribological Properties of Nano-Sized ZrO_2 Ceramic Particles in Automotive Lubricants. FME Transactions, 49(1).
[17] Pradeep, R., Kumar, B. P. and Prashanth, B. (2014). Evaluation of mechanical properties of aluminium alloy 7075 reinforced with silicon carbide and red mud composite. International Journal of Engineering Research and General Science, 2(6), pp. 1081-1088.
[18] Anitha, P. and Srinivas Rao, M. (2022). Influence of titanium diboride and graphite on microstructure characteristics and mechanical behaviors of aluminium hybrid nanocomposites. Proceedings of the Institution of Mechanical Engineers, Part E: Journal of Process Mechanical Engineering, 236(5), pp. 2071-2081.
[19] Moustafa, E. B. and Taha, M. A. (2023). The effect of mono and hybrid additives of ceramic nanoparticles on the tribological behavior and mechanical characteristics of an Al-based composite matrix produced by friction stir processing. Nanomaterials, 13(14), 2148.
[20] Singh, A. K., Yadav, G. and Gupta, P. (2023). Correlation of Structural and Mechanical Properties for Ultrasonically Stir Casted Al6061 Reinforced SiC-AlN Hybrid Metal Matrix Composites. ECS Journal of Solid State Science and Technology, 12(5), 057008.
[21] Madhukar, P., Selvaraj, N., Gujjala, R. and Rao, C. S. P. (2019). Production of high performance AA7150-1% SiC nanocomposite by novel fabrication process of ultrasonication assisted stir casting. Ultrasonics Sonochemistry, 58, 104665.
[22] Kok, M. (2005). Production and mechanical properties of Al_2O_3 particle-reinforced 2024 aluminium alloy composites. Journal of materials processing technology, 161(3), pp. 381-387.

[23] Hashim, J., Looney, L. and Hashmi, M. S. J. (1999). Metal matrix composites: production by the stir casting method. Journal of materials processing technology, 92, pp. 1-7.

[24] Singh, T., Tiwari, S. K. and Shukla, D. K. (2020). Effects of Al_2O_3 nanoparticles volume fractions on microstructural and mechanical characteristics of friction stir welded nanocomposites. Nanocomposites, 6(2), pp. 76-84.

[25] Bharath, V., Auradi, V., Kumar, G. V., Nagaral, M., Chavali, M., Helal, M. and Galal, A. M. (2022). Microstructural evolution, tensile failure, fatigue behavior and wear properties of Al2O3 reinforced Al2014 alloy T6 heat treated metal composites. Materials, 15(12), 4244.